PLOS ONE

RESEARCH ARTICLE

Expanding the geography of evapotranspiration: An improved method to quantify land-to-air water fluxes in tropical and subtropical regions

Daniela Jerszurki[1]*, Jorge L. M. Souza[2], Lucas C. R. Silva[3]

1 Wyler Department of Dryland Agriculture, French Associates Institute for Agriculture and Biotechnology of Drylands, Jacob Blaustein Institutes for Desert Research, Ben-Gurion University of the Negev, Sede Boqer, Israel, **2** Soil and Environment Studies Program, Federal University of Paraná, Curitiba, Paraná, Brazil, **3** Environmental Studies Program and Department of Geography, University of Oregon, Eugene, Oregon, United States of America

* danijerszurki@gmail.com

Citation: Jerszurki D, Souza JLM, Silva LCR (2017) Expanding the geography of evapotranspiration: An improved method to quantify land-to-air water fluxes in tropical and subtropical regions. PLoS ONE 12(6): e0180055. https://doi.org/10.1371/journal.pone.0180055

Editor: Ben Bond-Lamberty, Pacific Northwest National Laboratory, UNITED STATES

Received: November 14, 2016

Accepted: June 8, 2017

Published: June 28, 2017

Data Availability Statement: All relevant data are within the paper and its Supporting Information files.

Funding: DJ was supported by Coordination for the Improvement of Higher Education Personnel (CAPES/PDSE, Brazil) (https://www.capes.gov.br/) and Araucaria Foundation (http://www.fappr.pr.gov.br/).

Competing interests: The authors have declared that no competing interests exist.

Abstract

The development of new reference evapotranspiration (*ETo*) methods hold significant promise for improving our quantitative understanding of climatic impacts on water loss from the land to the atmosphere. To address the challenge of estimating *ETo* in tropical and subtropical regions where direct measurements are scarce we tested a new method based on geographical patterns of extraterrestrial radiation (*Ra*) and atmospheric water potential (Ψ_{air}). Our approach consisted of generating daily estimates of *ETo* across several climate zones in Brazil–as a model system–which we compared with standard ETo_{PM} (Penman-Monteith) estimates. In contrast with ETo_{PM}, the simplified method (ETo_{MJS}) relies solely on Ψ_{air} calculated from widely available air temperature (°C) and relative humidity (%) data, which combined with *Ra* data resulted in reliable estimates of equivalent evaporation (E_e) and *ETo*. We used regression analyses of Ψ_{air} *vs* ETo_{PM} and E_e *vs* ETo_{PM} to calibrate the ETo_{MJS} $_{(\Psi air)}$ and ETo_{MJS} estimates from 2004 to 2014 and between seasons and climatic zone. Finally, we evaluated the performance of the new method based on the coefficient of determination (R^2) and correlation (*R*), index of agreement "*d*", mean absolute error (*MAE*) and mean reason *(MR*). This evaluation confirmed the suitability of the ETo_{MJS} method for application in tropical and subtropical regions, where the climatic information needed for the standard ETo_{PM} calculation is absent.

Introduction

The amount of water that flows through the soil-plant-atmosphere continuum is a key factor to be considered in ecosystem conservation and management efforts. Estimates of water fluxes from land-to-air are needed, for example, for the introduction of new crops, prediction of migration of plant species, and improvement of soil and irrigation management under climate

change [1–3]. Assessing water fluxes in situ can be costly and time consuming and, depending on the method used, such assessments are subject to large uncertainties [4]. Baseline estimates of water fluxes are missing in many parts of the world, including the tropical and subtropical regions [5], owing to limited measurements of reference evapotranspiration (*ETo*).

Over the past 50 years, several methods have been developed to estimate the reference evapotranspiration [6–7]. The need to find a best model with minimum possible error relative to field measurements led to the Penman-Monteith model [6, 8–10], which is recognized as the standard method for agricultural regions worldwide [6, 9]. However, in areas that are dominated by natural ecosystems, especially those located in remote tropical and subtropical regions, the climate data needed for the application of the Penman-Monteith method are often unavailable [5]. Attempts to simplify the estimation of *ETo* using a small set of climatic variables, such air temperature and solar radiation, have been proposed [11–30]. The validation of simplified methods to estimate *ETo* has been mostly limited to climatic zones where they can be adjusted to fit Penman-Monteith projections, thus, overlooking vast tropical and subtropical regions [31–50].

In general, the literature that reports the performance of alternative methods against the standard Penman-Monteith method does so for specific climate conditions, missing the geographical variability of regional climates. This approach has proven inadequate for generating regional *ETo* estimates in countries that encompass multiple tropical and subtropical climatic conditions, such as Brazil [37–50]. The existing simplified *ETo* methods based on air temperature or on the combined effect of air temperature and solar radiation have shown either significant [39, 45] or not significant associations [48–49] to the Penman-Monteith method in tropical and subtropical climates. Those methods are thought to better match Penman-Monteith estimates in dry and warm climate zones [40, 50]. Under subtropical humid climates the methods based on solar radiation have shown the best adjustment to Penman-Monteith estimates [37, 41, 43]. Although those studies have contributed for the evaluation and choice of the most suitable *ETo* method within specific regions, they also show limitations for adequately estimating *ETo* across different climatic zones. Developing an alternative *ETo* method that is sensitive to regional climate heterogeneity in the tropics and sub-tropics is the central motivation of this study.

Among the most important climatic variables, vapor pressure deficit (*VPD*) exerts dominant influence on *ETo* estimations in different climate types [51–53]. However, for the coldest and wettest climates of tropical and subtropical regions in many parts of the world [51, 54–55], solar radiation also governs *ETo* variability. Thus, the use of solar radiation in combination to the *VPD* is a promising alternative to *ETo* estimates at scales that encompass multiple climatic regions. The solar radiation represents the total available latent energy to evapotranspiration process [56]. Among the existing radiation forms, the extraterrestrial radiation is easily estimated by use of latitude, hour of the day and solar constant (G_{cs}). In the Penman-Monteith method, evaporative fluxes are mainly attributed to *VPD* which is related to the aerodynamic terms, such as wind speed [6]. Vapor pressure deficit in combination with latent heat drive soil water evaporation [57] and plant transpiration [4]. Thus, the resulting evapotranspiration is proportional to VPD and energy inputs [58] and the combined analysis of these variables allows for the study of the spatial heterogeneity of *ETo* [58].

Notably, the flux of water from soil and plants to the atmosphere is a result of the water potential gradients, with movement occurring toward the direction of the lowest water potential [57]. On average, the water vapor in the atmosphere represents the lowest state of energy (i.e., lowest water potential) along the soil-plant-atmosphere system. The study of water movement in the atmosphere can be complicated due variation in plant cover [4], species-specific water-use efficiency and transpiration rates [59], variability in water vapor pressure in relation

to other gases, and climatic dynamism [60]. However, previous investigations of the water potential gradients along the soil-plant-atmosphere continuum have suggested that net water fluxes can be simplified to produce reliable *ETo* baselines that are important for management as well as conservation efforts aimed at mitigating the effects of climate change [57, 61–63]. Accordingly, here we propose an alternative *ETo* method based on atmospheric water potential and solar radiation, using a wide range of climate types in Brazil as a model system for improving tropical and subtropical land-to-air water flux estimates.

Theoretical considerations

The basic principle that surrounds the notion of atmospheric water potential as a driving force of evapotranspiration, regardless of plant cover and soil properties, is rooted in the first and second laws of thermodynamics [57, 61]. Briefly, the balance of heat, mechanical work (W), and variation of internal energy (ΔU) of a system are considered to be in equilibrium at time zero:

$$Q - W - \Delta U = 0 \tag{1}$$

where: Q is heat added to the system; W is the mechanical work; and, ΔU is the change in internal energy U of the system.

Considering changes in energy that trigger dynamic responses:

$$dU = dQ - dW \tag{2}$$

where: dU is a differential function of U, depending only of initial and final state of a transformation; dQ is the differential of line function, representing the input and outputs of heat; and, dW is the differential of work, equal to dQ in adiabatic processes.

dQ is equal to TdS, where S is the entropy. The definition of S from the initial equilibrium (A) to the dynamic (B) state is given by:

$$S_B - S_A = \int_A^B \frac{dQ}{T} \tag{3}$$

Considering the second law of thermodynamics, which defines other energy functions of thermodynamic potential, the Gibbs free energy function is given by:

$$G = H - T \cdot S = U + P \cdot V - T \cdot S \tag{4}$$

The Gibbs free energy (G) is only dependent on the system state, i.e., the pressure (P), volume (V) and temperature (T). This function explains the available energy to make work, which is given by:

$$dG = V \cdot dP - S \cdot dT \tag{5}$$

where: G is a function of T and P. Representing the Eq (5) in a mass (m) basis, considering $P = e_a$ and $g = \Psi$ in an isothermal path ($dT = 0$) and assuming the water vapor acting as an ideal gas we have:

$$d\psi = \frac{R \cdot T}{Mv} \cdot \frac{de_a}{e_a} \tag{6}$$

Integrating the equation from standard condition (e_s) to actual condition (e_a) we have:

$$\Delta\psi_{air} = \int_{e_s}^{e_a} \frac{R \cdot T}{Mv} \cdot \frac{de_a}{e_a} = \frac{R \cdot T}{Mv} \cdot \ln\left(\frac{e_a}{e_s}\right) \quad (7)$$

Due to the difficult of measurement of the absolute Ψ_{air}, between the standard (Ψ_o) and interest condition (Ψ_{air}), we set $\Psi_o = 0$ and $\Delta\Psi_{air} = \Psi_{air}$:

$$\psi_{air} = \frac{R \cdot T}{Mv} \ln\left(\frac{e_a}{e_s}\right) \quad (8)$$

where: Ψ_{air} is the atmospheric water potential (MPa); R is the gas constant (8.314 J mol^{-1} K^{-1}); T is the absolute temperature (K); e_a is the actual vapor pressure (MPa); e_s is the saturated vapor pressure (MPa); and, Mv is the partial molar volume of water (18.10^{-6} m^3 mol^{-1}).

In order to combine the effect of Ψ_{air} to extraterrestrial radiation (Ra) in the equivalent water evaporation, the Ψ_{air} is turned into a coefficient of proportionality $K_{\Psi air}$, ranging from 0 to 1:

$$K_{\psi air} = \left| \frac{\psi_{air.i} - \psi_{air.\min}}{\psi_{air.\max} - \psi_{air.\min}} \right| \quad (9)$$

where: $K_{\Psi air}$ is the coefficient of proportionality of Ψ_{air} (dimensionless); $\Psi_{air.i}$ is the atmospheric water potential at the i-day (MPa); $\Psi_{air.max}$ is the maximum atmospheric water potential at the analyzed period (MPa); $\Psi_{air.min}$ is the minimum atmospheric water potential at the analyzed period (MPa).

The equivalent water evaporation (E_e–mm d^{-1}) is obtained by transformation of Ra (MJ m^{-2} d^{-1}) by use of the inverse constant of the latent heat of vaporization (1/λ) [6] multiplied by $K_{\Psi air}$.

$$Ra = \frac{24 \cdot (60)}{\pi} \cdot G_{sc} \cdot dr \cdot [\omega_s \cdot sen\,(\varphi) \cdot sen\,(\delta) + \cos\,(\varphi) \cdot \cos\,(\delta) \cdot sen\,(\omega_s)] \quad (10)$$

$$E_e = K_{\psi air} \cdot \frac{R_a}{\lambda} \quad (11)$$

where: Ra is the extraterrestrial radiation (MJ m^{-2} d^{-1}); G_{sc} is the solar constant (G_{sc} = 0.0820 MJ m^{-2} min^{-1}); dr is the relative distance Earth–Sun (dimensionless); ω_s is the hourly angle corresponding to sunset (rad); φ is the latitude (rad); δ is the inclination of the sun (rad); E_e is the equivalent water evaporation obtained by solar radiation and weighted by atmospheric water potential at each i-day (mm d^{-1}); $K_{\Psi air}$ is the coefficient of proportionality of atmospheric water potential (dimensionless); λ is the latent heat of vaporization (λ = 2.45 MJ kg^{-1}). The estimated E_e can then be converted into ETo as explained in the calibration step described below.

Material and methods

Climate data

To perform the calculations described above in Brazil as a case study we used a set of nine meteorological stations [64] (Table 1) distributed across the most representative climatic zones of that country (Table 2) [65]. We relied on daily observations of maximum, minimum, and average air temperature (°C), relative humidity (%), daily sunshine hours (MJ m^{-2} d^{-1}), and wind speed (m s^{-1}) measured at ten meters above the ground level, from January 2004 to

Table 1. Climate classification, location and coordinates of the Brazilian meteorological stations used in this study.

Climate	State	Station	Latitude (degree S)	Longitude (degree W)	Altitude (m)
Af	Amazonas	Manaus	–3.10	–60.01	61.25
Am	Amapá	Macapá	–0.05	–51.11	14.46
As	Sergipe	Aracaju	–10.95	–37.01	4.72
Aw	Goiás	Goiânia	–16.66	–49.25	741.48
Bsh	Pernambuco	Petrolina	–9.38	–40.48	370.46
Cfa	Rio Grande do Sul	Porto Alegre	–30.05	–51.16	46.97
Cfb	Paraná	Curitiba	–25.43	–49.26	923.50
Cwa	Minas Gerais	Uberaba	–19.73	–47.95	737.00
Cwb	Minas Gerais	Belo Horizonte	–19.93	–43.93	915.00

https://doi.org/10.1371/journal.pone.0180055.t001

January 2014. Daily sunshine hours were measured by the heliograph Campbell-Stokes (model 240-1070-L) at hourly intervals. Daily wind speed was obtained by the anemometer Vaisala WT521. Wind speed measurements were transformed to wind speed at 2 m height by the wind profile relationship [6]. Daily air temperature and relative humidity were obtained by the thermometer Fluke 5699 and the humidity sensor Vaisala HMK15, respectively.

Penman-Monteith reference evapotranspiration (ETo_{PM})

The Penman-Monteith method estimates ETo as follows [9]:

$$ETo_{PM} = \frac{0,408 \cdot \Delta \cdot (R_n - G) + \gamma_{psy} \cdot \frac{C_n}{(T_{air}+273)} \cdot u_2 \cdot (e_s - e_a)}{\Delta + \gamma_{psy} \cdot (1 + C_d \cdot u_2)} \quad (12)$$

where: ETo_{PM}–reference evapotranspiration (mm d^{-1}); Δ–slope of the saturated water-vapor-

Table 2. Koeppen's climate classification based on temperature and precipitation at each location.

Symbol	Temperature (°C)			Rainfall (mm)			Climate
				Monthly		Annual	
	T_1	T_2	T_3	R_d	R_w		
Af	≥ 18			≥60		≥25(100–R_d)	Tropical without dry season
Am					< 60		Tropical monsoon
As						<25(100–R_{sdry})	Tropical with dry summer
Aw						<25(100–R_{wdry})	Tropical with dry winter
Bsh			≥18			<5.R_{LIM}	Semi-arid with low latitude and altitude
Cfa	–3<T<18	≥22		>40			Humid subtropical, oceanic climate without dry season and with hot summer
Cfb		4≤T_{M10}<22					Humid subtropical, oceanic climate without dry season, with temperate summer
Cwa	–3<T<18	≥22		<40			Humid subtropical with dry winter and hot summer
Cwb		4≥T_{M10}<22			R_{swet}≥10. R_{wwet}		Humid subtropical with dry winter and temperate summer

T1 –temperature of the coldest month;T2 –temperature of the hottest month; T3 –annual mean temperature; Rd–rainfall of the driest month; Rw–rainfall of the wettest month; R_{sdry}–rainfall of the driest month on summer; Rwdry–rainfall of the driest month on winter; R_{swet}–rainfall of the wettest month on summer; R_{wwet}–rainfall of the wettest month on winter; R_{LIM}–rainfall of the driest month of the year; T_{M10} –number of months where the temperature is above 10°C.

https://doi.org/10.1371/journal.pone.0180055.t002

pressure curve (kPa $^{o}C^{-1}$); R_n–net radiation at the crop surface (MJ m^{-2} d^{-1}); G–soil heat flux (MJ m^{-2} d^{-1}); γ_{psy}–psychrometric constant (kPa $^{o}C^{-1}$); T_{air}–average daily air temperature (^{o}C); u_2 –wind speed at two meters height (m s^{-1}); e_s–saturated vapor pressure (kPa); e_a–actual vapor pressure (kPa); C_n–constant related to the reference type and calculation time step, considered equal to 900 for grass (dimensionless); C_d–constant related to the reference type and calculation time step, considered equal to 0.34 for grass (dimensionless).

Daily vapor pressure deficit (e_s–e_a) is estimated by the difference between saturated and actual vapor pressure. Saturated vapor pressure is calculated using air temperature based on the Tetens formula [66]. Actual vapor pressure is obtained by saturated vapor pressure multiplied by fractional humidity. Daily net radiation (*Rn*) is estimated by the difference between net longwave and shortwave radiation. The net longwave radiation (*Rnl*) is obtained by relative shortwave radiation (*Rs*/*Rso*), air temperature and actual vapor pressure. The net shortwave radiation (*Rns*) is obtained from solar radiation (*Rs*) measurements, which are determined by the relation between extraterrestrial radiation (*Ra*) and relative sunshine duration (*n*/*N*) [6]. Finally, soil heat flux (*G*) is calculated using air temperature [67].

Alternative "Moretti-Jerszurki-Silva" method: $ETo_{MJS(\Psi air)}$ and ETo_{MJS}

The alternative "Moretti-Jerszurki-Silva" method is easily calibrated and used to estimate the *ETo*. The method is proposed based on Ψ_{air} ($ETo_{MJS(\Psi air)}$); and, on Ψ_{air} and *Ra* by estimation of E_e (ETo_{MJS}). Daily values of Ψ_{air} (Eq 8) *vs* ETo_{PM} and E_e (Eq 11) *vs* ETo_{PM} obtained from meteorological stations are adjusted from regression analysis in a monthly and annual basis, between 2004 and 2011. As a general practice in validation procedures, an independent dataset should be used to fit the model; accordingly, the performance assessment and validation of $ETo_{MJS(\Psi air)}$ and ETo_{MJS} against ETo_{PM} are determined based on regression analysis for the last two years of the time series (January of 2012 –January of 2014). $ETo_{MJS(\Psi air)}$ and ETo_{MJS} values are obtained using coefficients "*a*" and "*b*" for Ψ_{air} *vs* ETo_{PM} and E_e *vs* ETo_{PM}, respectively, between 2004 and 2011.

$$ETo_{MJ(\psi air)\ i} = a + b.\ \psi_{air\ i} \tag{13}$$

$$ETo_{MJ\ i} = a + b.\ E_e \tag{14}$$

where: $ETo_{MJS(\Psi air).i}$ is the calibrated reference evapotranspiration estimated by atmospheric water potential at each *i*-day (mm d^{-1}); $\Psi_{air.i}$ is the atmospheric water potential at each *i*-day (MPa); $ETo_{MJS.i}$ is the calibrated reference evapotranspiration estimated by atmospheric water potential and solar radiation at each *i*-day (mm d^{-1}); E_e is the equivalent evaporation obtained by solar radiation and weighted by atmospheric water potential at each *i*-day (mm d^{-1}); *a* is the linear coefficient (mm d^{-1}); *b* is the angular coefficient (dimensionless).

Validation of $ETo_{MJS(\Psi air)}$ and ETo_{MJS} estimates using lysimetric measurements

In addition to the 10-years comparison with standard ETo_{PM} in multiple climatic zones, described above, a seasonal validation of the new $ETo_{MJS(\Psi air)}$ and ETo_{MJS} method was conducted in situ using available lysimetric measurements (ETo_{LIS}) located at a reference pasture plantation. This independent validation was performed at a site of typical semi-arid climate type *Bsh* (latitude 3°18'S, longitude 39°12'W at an altitude of 30 m above the sea level) using climatic data collected between 1997 and 1998 as well ETo_{LIS} previously reported in the literature [68]. The validation could only be performed at this site and period due to the scarcity of co-located ETo_{LIS} and reliable weather stations in other climatic regions. This is sufficient,

however, to demonstrate that the proposed method holds in the analysis of both seasonal and multi-year *ET* patterns without the need for the detailed climatic data that is required for the standard ETo_{PM} calculation. As described above, the new $ETo_{MJS(\Psi air)}$ (Eqs 8 and 13) and ETo_{MJS} (Eqs 8–11 and 14) were estimated using only air temperature, relative humidity and altitude. The calibration of $ETo_{MJS(\Psi air)}$ (Eq 13) and ETo_{MJS} (Eq 14) were carried out using the monthly coefficients "*a*" and "*b*" of the linear relation between Ψ_{air} *vs* ETo_{PM} (March: $a = 2.39$ mm d^{-1} and $b = -0.043$; April: $a = 2.59$ mm d^{-1} and $b = -0.036$; May: $a = 2.20$ mm d^{-1} and $b = -0.035$; and, June: $a = 2.09$ mm d^{-1} and $b = -0.033$), and E_e *vs* ETo_{PM} (March: $a = 2.74$ mm d^{-1} and $b = 0.47$; April: $a = 2.84$ mm d^{-1} and $b = 0.44$; May: $a = 2.44$ mm d^{-1} and $b = 0.48$; and, June: $a = 2.34$ mm d^{-1} and $b = 0.47$), obtained in the present study for the semi-arid climate subgroup, between 2004–2011. Finally, $ETo_{MJS(\Psi air)}$ and ETo_{MJS} were regressed against ETo_{LIS}.

Statistics

We used coefficients of variation (CV) to assess the variability of ETo_{PM} in response to climatic data collected across sites between 2004 and 2014. We relied on multiple regression analyses to correlate the estimated ETo_{PM} to climatic variables for each specific climatic zone (Table 1). We then compared daily reference evapotranspiration obtained with the alternative method to standard daily ETo_{PM} and/or ETo_{LIS} (validation) using regression analysis. The goodness of fit of the alternative methods was obtained by use of R^2 and *R* as an index of precision and correlation, and agreement index "*d*" as an index of accuracy [69]. The agreement index is a measure of the effectiveness with which the alternative method estimates the Penman-Monteith reference evapotranspiration, considering the dispersion of the data relative to the 1:1 line:

$$d = 1 - \left[\frac{\sum_{i=1}^{n} (ETo_{alternativei} - ETo_i)^2}{\sum_{i=1}^{n} (|ETo_{alternativei} - \overline{ETo}| + |ETo_i - \overline{ETo}|)^2} \right] \quad (15)$$

where: *d* is the agreement index (dimensionless); $ETo_{alternative.i}$ is the reference evapotranspiration estimated by alternative method at each *i*-day (mm d^{-1}); $ETo._i$ is the reference evapotranspiration estimated by Penman-Monteith method or measured in the lysimeters at each *i*-day (mm d^{-1}); $\overline{ETo}$ is the average reference evapotranspiration estimated by Penman-Monteith method or measured in the lysimeters (mm d^{-1}).

For further comparison, the mean absolute error (*MAE*) and the mean ratio (*MR*) [70] were used to evaluate the reference evapotranspiration estimated by atmospheric water potential:

$$MAE = \frac{1}{n} \cdot \sum_{i=1}^{n} (|ETo_{alternativei} - ETo_i|) \quad (16)$$

$$MR = \frac{1}{n} \sum_{i=1}^{n} \frac{ETo_{alternativei}}{ETo_i} \quad (17)$$

where: $ETo_{alternative.i}$ is the reference evapotranspiration estimated by the alternative method at each *i*-day (mm d^{-1}); ETo_i is the reference evapotranspiration estimated by Penman-Monteith method or measured in the lysimeters at each *i*-day (mm d^{-1}); *n* is the number of observations (dimensionless). Finally, *MAE* was used to measure the accuracy of the proposed method and *MR* was used as an index of under- or overestimation of the standard ETo_{PM}, such that when standard and alternative data are similar, *MAE* is close to zero and *MR* is close to one, indicating a more accurate estimation.

Results

As expected, our observations showed large variability of all climatic parameters (T_{max}, T_{min}, *RH*, *Rs*, u_2 and *VPD*) across the different climate zones sampled throughout Brazil. The results described here span *ETo* trends in humid subtropical, tropical with dry summers, and semi-arid regions (Table 3). In general, *VPD* was the most seasonally variable parameter in humid climatic zones, reaching its lowest values during wet summers. Across sites, high T_{max} and T_{min} and low *RH* in semi-arid climate resulted in the highest *VPD* and ETo_{PM}. These results reflect the geographical influence–governed by variation in atmospheric water potential and *Rs*–on *ETo* throughout the country.

Adjustment of atmospheric water potential and performance of the alternative methods $ETo_{MJS(\Psi air)}$ and ETo_{MJS}

We identified a strong negative linear relationship between Ψ_{air} and ETo_{PM} ($P<0.05$), with the coefficients "*a*" and "*b*" varying with climatic zone (S1 Fig). The linear coefficient "*a*" corresponds to other climatic variables that in addition to Ψ_{air} drive atmospheric water demand (*VPD*) and control ETo_{PM}, while coefficient "*b*" corresponds to the rate of change in the ETo_{PM} relative to Ψ_{air}. Even though Ψ_{air} is not used in the calculation of the standard ETo_{PM} (Eq 12), it strongly affects its variability over time and space. The exception occurred at the humid subtropical site, which showed the smallest linear coefficients between Ψ_{air} and ETo_{PM}, due to lower magnitudes of ETo_{PM}. We also identified an *ETo* threshold (2 mm d^{-1}) beyond which evapotranspiration is primarily controlled by solar radiation and wind speed (S1 Fig). The highest angular coefficients |"*b*"| were observed in the tropical climate with dry winter (Aw) and the lowest in the subtropical climate. Accordingly, stronger associations and lower errors of adjustment in $ETo_{MJS(\Psi air)}$ were observed for tropical and semi-arid climates (S2 Fig and Table 4). Across all climate zones, the lowest associations between $ETo_{MJS(\Psi air)}$ and ETo_{PM} were observed during dry winter months (Fig 1).

We also identified a linear relationship ($P<0.05$) between E_e and ETo_{PM} (S3 Fig), which demonstrates the suitability of using Ψ_{air} and *Ra*–sole drivers of E_e–as the key parameters in the alternative method. The linear coefficients "*a*" were around: 3 mm day^{-1} for the semi-arid climate; 1.5 to 2.5 mm day^{-1} for tropical climates; and 1.0 to 2.5 mm day^{-1} for subtropical climates. The angular coefficients | "*b*" | ranged from 0.35 to 0.5 for subtropical climates; 0.4 for the semi-arid climate; and between 0.27 and 0.33 for tropical climates (S3 Fig). The calibration process, which involved the relation between E_e and ETo_{PM}, further improved the performance of the alternative method ETo_{MJS} for subtropical climates (Fig 1, S4 Fig and Table 4).

The smallest adjustment errors (MAE and MR) of $ETo_{MJS(\Psi air)}$ and ETo_{MJS} were observed in the tropical climate types (Table 4). The smallest associations between ETo_{MJS} *vs* ETo_{PM} were observed in winter months, which is to be expected given the relatively low *Ra* and ETo_{PM} typical of this season [71].

In an attempt to establish generic "*a*" and "*b*" coefficients for the different climate zones and seasons, we used the linear and angular coefficients determined at the three main climate groups: tropical, semi-arid and sub-tropical. This resulted in a predictable ET trend response to Ψ_{air} and E_e. The highest significant $ETo_{MJS(\Psi air)}$ and ETo_{MJS} associations with ETo_{PM} were observed when using monthly average coefficients for the climate subgroups: humid tropical (Af, Am, As and Aw), semi-arid (*Bsh*), humid subtropical without dry season (Cfa and Cfb) and humid subtropical climates with dry summers (Cwa and Cwb) (Fig 2).

Table 3. Annual daily average, coefficient of variation of climatic variables and coefficient of correlation between ETo_{PM} and climatic variables between 2004 and 2014 at different climatic zones.

Clim	Variable	Aver	CV (%)					R (dimensionless)				
			A	Sum	Aut	Win	Spr	A	Sum	Aut	Win	Spr
Af	T_{min} (°C)	22.74	2.64	1.34	1.54	1.61	1.50	0.2	0.0	0.6	0.1	-0.1
	T_{max} (°C)	29.83	2.42	1.33	1.75	1.97	1.45	0.7	0.2	0.8	0.7	0.2
	RH (%)	73.77	3.14	1.89	1.88	2.52	2.05	-0.5	-0.2	-0.3	-0.8	-0.5
	VPD (kPa)	0.66	13.00	4.71	6.59	10.80	7.40	0.8	0.7	0.7	0.9	0.7
	Rs (MJ m^{-2} d^{-1})	18.06	9.54	3.17	7.53	8.51	3.47	1.0	0.9	1.0	1.0	0.9
	u_2 (m s^{-1})	1.73	8.45	6.00	6.11	7.00	6.79	0.2	0.3	-0.3	0.3	0.5
	ETo_{PM} (mm d^{-1})	3.73	11.10	3.37	8.67	9.97	3.22	–	–	–	–	–
Am	T_{min} (°C)	22.22	4.03	0.48	2.94	1.71	1.63	0.5	-0.1	1.0	0.8	0.5
	T_{max} (°C)	30.37	2.31	0.49	2.06	1.31	0.80	0.6	-0.1	1.0	0.9	0.6
	RH (%)	79.02	2.30	0.49	0.98	2.09	1.05	-0.5	-0.6	-0.9	-1.0	0.0
	VPD (kPa)	0.76	10.96	2.34	8.02	9.93	2.81	0.6	0.5	1.0	1.0	0.9
	Rs (MJ m^{-2} d^{-1})	18.56	10.13	2.53	6.97	8.05	2.08	0.6	0.9	1.0	1.0	0.9
	u_2 (m s^{-1})	1.98	13.84	3.89	7.19	11.90	2.86	0.6	0.7	0.9	1.0	0.6
	ETo_{PM} (mm d^{-1})	3.97	15.71	14.24	9.84	10.74	2.27	–	–	–	–	–
As	T_{min} (°C)	23.41	4.52	0.87	2.26	1.83	2.03	0.7	0.7	0.9	0.6	0.3
	T_{max} (°C)	30.01	2.14	0.33	1.44	0.93	0.86	0.7	0.6	0.9	0.9	0.3
	RH (%)	78.41	3.95	1.71	1.07	3.02	0.85	-0.9	-0.9	-0.8	-1.0	-0.7
	VPD (kPa)	0.78	16.46	6.67	7.21	11.90	2.57	1.0	0.9	0.9	1.0	0.8
	Rs (MJ m^{-2} d^{-1})	21.04	11.49	3.76	5.55	10.29	2.32	1.0	0.9	0.9	1.0	0.9
	u_2 (m s^{-1})	3.14	14.53	8.26	7.07	8.90	5.50	0.7	0.8	-0.7	0.9	0.4
	ETo_{PM} (mm d^{-1})	4.45	14.12	4.46	6.85	12.33	2.40	–	–	–	–	–
Aw	T_{min} (°C)	20.68	7.42	0.52	5.76	6.13	1.27	0.7	0.7	0.1	0.7	-0.2
	T_{max} (°C)	31.45	3.23	0.70	1.22	3.66	2.06	0.8	0.7	0.5	0.8	0.3
	RH (%)	71.74	11.27	1.67	4.76	6.84	6.80	-0.9	-0.8	-0.6	-0.9	-0.7
	VPD (kPa)	0.98	31.28	8.09	12.58	16.88	17.82	0.9	0.8	0.6	0.9	0.7
	Rs (MJ m^{-2} d^{-1})	18.98	6.87	3.02	3.09	6.23	3.38	1.0	0.9	0.9	1.0	0.9
	u_2 (m s^{-1})	1.47	12.39	6.61	7.39	8.57	5.45	0.9	0.7	0.4	0.9	0.0
	ETo_{PM} (mm d^{-1})	4.09	12.83	4.17	4.02	12.49	5.68	–	–	–	–	–
Bsh	T_{min} (°C)	22.01	5.86	0.97	3.74	2.32	2.63	0.5	0.3	0.8	0.5	0.4
	T_{max} (°C)	32.14	4.66	1.22	2.50	3.58	1.29	0.9	0.7	0.9	0.9	0.6
	RH (%)	55.37	10.49	5.20	2.73	8.18	6.55	-0.8	-0.8	0.4	-0.9	-0.2
	VPD (kPa)	1.59	18.44	11.93	6.26	15.94	4.78	0.9	0.8	0.4	0.9	0.5
	Rs (MJ m^{-2} d^{-1})	17.71	11.98	4.13	8.55	10.75	3.19	0.9	0.7	0.9	0.9	0.7
	u_2 (m s^{-1})	2.28	12.34	8.36	10.05	6.23	6.82	0.0	0.8	-0.5	0.4	0.2
	ETo_{PM} (mm d^{-1})	4.28	16.12	8.21	7.50	15.00	3.51	–	–	–	–	–
Cfa	T_{min} (°C)	16.44	20.84	2.11	15.70	8.00	9.06	0.9	0.1	1.0	0.8	0.9
	T_{max} (°C)	24.93	13.94	1.88	10.23	4.32	7.57	0.9	0.5	1.0	0.8	1.0
	RH (%)	78.51	3.50	2.16	2.40	2.26	2.51	-0.9	-0.8	-0.9	-0.8	-0.9
	VPD (kPa)	0.57	30.30	7.98	22.72	13.88	17.42	1.0	0.9	1.0	0.8	1.0
	Rs (MJ m^{-2} d^{-1})	17.01	26.51	8.14	17.88	18.17	9.80	1.0	1.0	1.0	1.0	1.0
	u_2 (m s^{-1})	2.57	19.84	9.01	14.01	16.28	6.30	0.8	0.7	0.9	0.9	0.2
	ETo_{PM} (mm d^{-1})	3.14	37.78	8.91	27.66	26.88	14.01	–	–	–	–	–
Cfb	T_{min} (°C)	13.08	2.57	2.57	2.57	2.57	2.57	0.9	0.2	1.0	0.7	0.9
	T_{max} (°C)	23.43	23.53	2.57	19.05	10.74	9.92	0.9	0.3	1.0	0.8	0.9
	RH (%)	81.22	11.33	2.03	8.88	5.09	7.14	-0.2	-0.5	-0.1	-0.5	-0.8
	VPD (kPa)	0.44	2.46	1.35	1.26	2.91	2.27	0.9	0.5	0.9	0.8	0.9
	Rs (MJ m^{-2} d^{-1})	16.31	19.44	7.23	14.55	16.53	15.99	1.0	1.0	1.0	1.0	1.0
	u_2 (m s^{-1})	2.10	20.53	6.66	14.17	13.60	8.99	0.7	0.5	0.5	0.6	0.5
	ETo_{PM} (mm d^{-1})	2.78	12.64	7.50	8.56	9.49	6.36	–	–	–	–	–

(*Continued*)

Table 3. (*Continued*)

Clim	Variable	Aver	CV (%)					R (dimensionless)				
			A	Sum	Aut	Win	Spr	A	Sum	Aut	Win	Spr
Cwa	T_{min} (°C)	17.12	16.96	4.00	15.24	14.32	5.75	0.5	-0.2	0.7	0.9	-0.3
	T_{max} (°C)	29.95	6.28	4.08	5.74	7.66	4.73	0.7	0.5	0.7	0.9	0.4
	RH (%)	65.88	15.21	4.37	7.30	13.39	11.79	-0.3	-0.7	0.3	-0.7	-0.7
	VPD (kPa)	1.06	30.15	14.98	12.74	23.38	26.75	0.5	0.7	0.3	0.9	0.7
	Rs (MJ m^{-2} d^{-1})	18.69	13.04	9.63	11.14	11.36	11.71	0.9	0.8	0.9	1.0	0.8
	u_2 (m s^{-1})	1.11	41.10	31.42	36.95	31.37	33.95	0.4	0.1	0.3	0.9	0.4
	ETo_{PM} (mm d^{-1})	3.86	19.91	12.06	15.92	20.90	13.09	—	—	—	—	—
Cwb	T_{min} (°C)	17.38	11.30	1.44	10.14	6.86	3.35	0.9	0.6	1.0	0.9	0.2
	T_{max} (°C)	27.21	5.20	1.98	4.79	4.30	1.96	0.9	0.5	1.0	0.9	0.6
	RH (%)	68.10	7.52	3.31	2.96	4.98	6.60	0.3	-0.6	0.7	-0.7	-0.2
	VPD (kPa)	0.92	13.67	10.09	5.78	13.62	14.77	0.3	0.6	0.7	0.9	0.4
	Rs (MJ m^{-2} d^{-1})	18.52	12.58	5.78	9.38	9.65	5.34	1.0	1.0	1.0	1.0	0.9
	u_2 (m s^{-1})	1.50	10.37	9.04	6.41	11.05	8.96	0.5	0.7	0.4	0.9	0.1
	ETo_{PM} (mm d^{-1})	3.61	18.81	5.94	15.10	17.60	5.23	—	—	—	—	—

Clim–climate type; Aver–annual daily average; A–annual; Sum–summer; Aut–autumn; Win–winter; Spr–spring.

https://doi.org/10.1371/journal.pone.0180055.t003

Validation of the alternative method "Moretti-Jerszurki-Silva": $ETo_{MJS(\Psi air)}$ and ETo_{MJS}

For the *in situ* validation, performed at the semiarid climate type *Bsh*, we identified a strong linear relationship ($P<0.05$) between Ψ_{air} and ETo_{LIS}, which further supports the relationship identified between ETo and Ψ_{air} across all climatic zones (S1 Fig). We also identified strong agreement in the $ETo_{MJS(\Psi air)}$ and ETo_{MJS} estimated with respect to their monthly coefficients "*a*" and "*b*" (Fig 3 and Table 5). The highest error of adjustment obtained for ETo_{MJS} (MAE = 0.65 mm d^{-1}) resulted in only 10% maximum overestimation of ETo_{LIS} at the reference site.

Discussion

Our results demonstrate that extraterrestrial radiation and atmospheric water potential can be used to reliably estimate *ETo* in tropical and subtropical regions. The influence of other

Table 4. Performance of $ETo_{MJS(\Psi air)}$ and ETo_{MJS} as assessed based on *R* (coefficient of correlation), *d* (agreement index), *MAE* (mean absolute error), and *MR* (mean ratio) for all climate zones in an annual basis, between 2012 and 2014.

Climate	R		"d" Index		MAE		MR	
	(dimensionless)				(mm d^{-1})		(dimensionless)	
	$ETo_{MJS(\Psi air)}$	ETo_{MJS}	$ETo_{MJS(\Psi air)}$	ETo_{MJS}	$ETo_{MJS(\Psi air)}$	ETo_{MJS}	$ETo_{MJS(\Psi air)}$	ETo_{MJS}
Af	0.82	0.84	0.88	0.87	0.45	0.47	1.10	1.11
Am	0.91	0.91	0.95	0.95	0.34	0.33	1.03	1.03
As	0.82	0.87	0.90	0.93	0.43	0.35	1.03	1.02
Aw	0.84	0.84	0.91	0.92	0.40	0.40	1.03	1.03
Bsh	0.81	0.88	0.88	0.92	0.58	0.46	0.99	0.99
Cfa	0.71	0.89	0.77	0.94	1.07	0.62	1.16	1.06
Cfb	0.61	0.84	0.69	0.90	0.77	0.51	1.09	1.04
Cwa	0.58	0.75	0.67	0.82	0.79	0.64	1.02	0.99
Cwb	0.48	0.77	0.57	0.84	0.70	0.57	1.11	1.11

https://doi.org/10.1371/journal.pone.0180055.t004

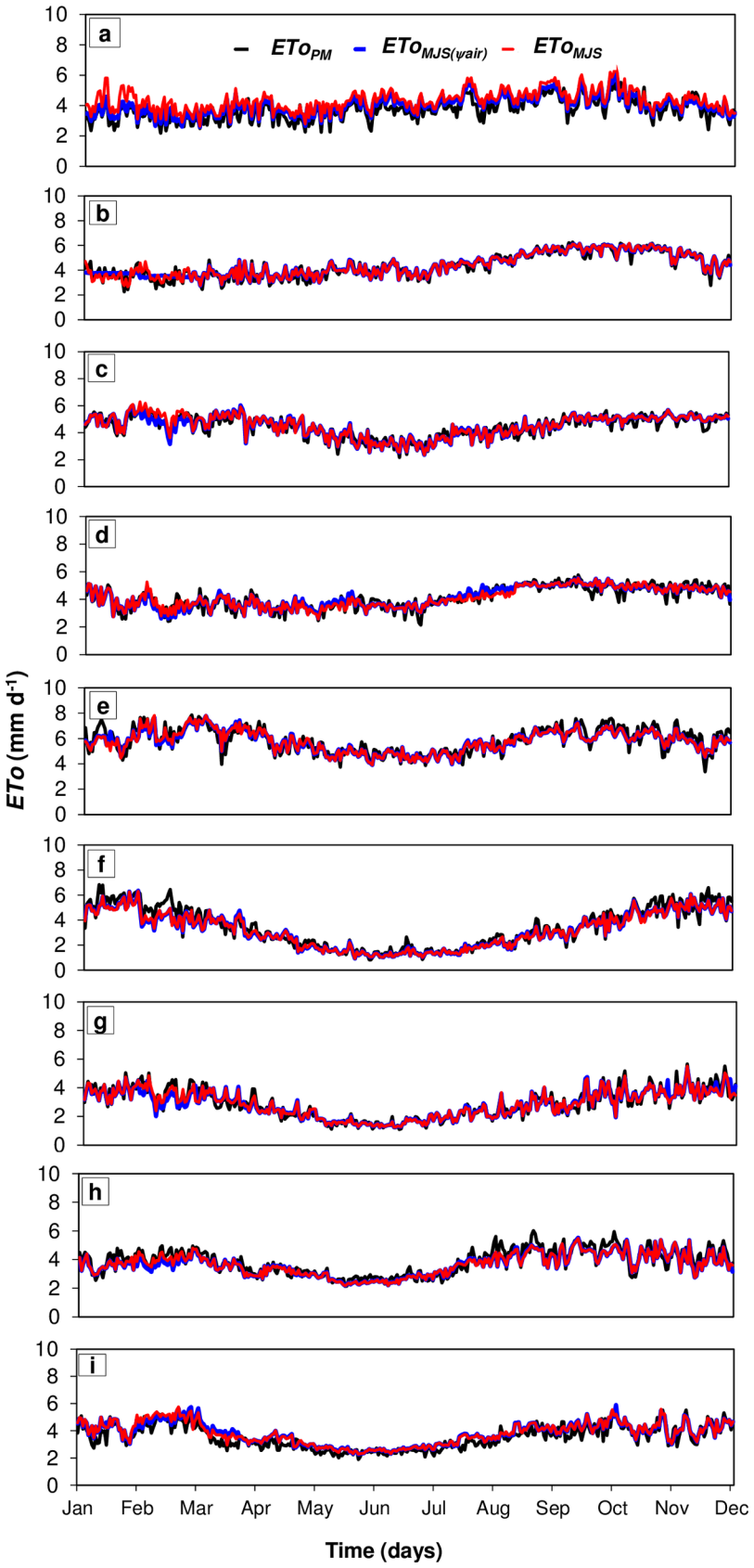
a
b
c
d
e
f
g
h
i
ETo_{PM}
$ETo_{MJS(\psi air)}$
ETo_{MJS}
ETo (mm d-1)
0
2
4
6
8
10
Jan
Feb
Mar
Apr
May
Jun
Jul
Aug
Sep
Oct
Nov
Dec
Time (days)

Fig 1. Daily reference evapotranspiration estimated by $ETo_{MJS(\Psi air)}$ and ETo_{MJS} alternative methods, between 2012 and 2014, for the climate types: (a) Af; (b) Am; (c) As; (d) Aw; (e) Bsh; (f) Cfa; (g) Cfb; (h) Cwa; and, (i) Cwb.

https://doi.org/10.1371/journal.pone.0180055.g001

climatic variables needed for the standard ETo_{PM} calculation, such as *Rs* and u_2, was indirectly but sufficiently accounted for in the analysis of radiation and atmospheric water potential, as evidenced by the strong agreement identified between ETo_{PM} and ETo_{MJS} estimates. Previous studies have shown similar results in cold and wet climates [54–55]; however, in our analysis of subtropical climates, the response of *ETo* to changes in Ψ_{air} indicates lower sensitivity relative to that observed in warmer and drier climates. In colder and wetter climatic zones, where atmospheric water demand is low (Table 4), *ETo* estimates were most strongly associated with *Rs* and u_2 [72].

In tropical and semi-arid climates 1 MPa of variation in Ψ_{air} led to strong (up to 0.0861 mm d^{-1}) ETo_{PM} responses. Similarly, we observed high sensitivity of the $ETo_{MJS(\Psi air)}$ method in response to air temperature and *RH*, which are the key variables controlling Ψ_{air} and used in climate classification systems [65]. This result was also confirmed in the analysis of "*a*" and "*b*" coefficients in warm climates (S1 Fig). Thus, the new simplified methods showed its best performances in warm and dry climatic zones (Fig 1 and S2 Fig)–with smaller errors of adjustment (R = 0.81 to 0.91; MAE: 0.34 to 0.58 mm d^{-1}; and, "*d*" index = 0.88 to 0.95) than observed for subtropical climates (R = 0.48 to 0.71; MAE: 0.7 to 1.07 mm d^{-1}; and, "*d*" index = 0.57 to 0.77). Considering the data spread of new and standard *ETo* estimates (relative to the 1:1 line in S2 Fig) our simplified method underestimated the ETo_{PM} by 1% in the semi-arid climate and overestimated the ETo_{PM} by up to 10% in the tropical climates and up to 16% in the subtropical climates (Table 4). Despite the high *Rs* observed in the semi-arid climate, the influence of *VPD* on ETo_{PM} was the most important, which is expected given the predominant warm and dry conditions [73–75], which led to strong agreement between $ETo_{MJS(\Psi air)}$ and ETo_{PM} at daily to seasonal scales.

In a previous study, the performance of 12 alternative *ETo* methods evaluated in 28 locations in central-western Brazil [46], the agreement ("*d*" index) of *ETo* obtained based on solar radiation (relative to the standard ETo_{PM}) ranged from 0.32 to 0.91. In contrast, the agreement obtained here with the proposed ETo_{MJS} method ranged from 0.92 to 0.95 across the same climatic regions. Moreover, the ETo_{MJS} agreement index was higher ("*d*" index = 0.92 to 0.95) than observed with other alternative methods ("*d*" index = 0.50 to 0.82) [47]. Therefore, the use of solar radiation in the alternative methods significantly improved *ETo* estimates. Notably, we also observed higher associations between ETo_{MJS} and ETo_{PM} (R = 0.84 to 0.89) than reported in previous studies (R = 0.76 to 0.83) in subtropical humid climate of southern Brazil [41, 43]. In general, compared to the method based on atmospheric water potential ($ETo_{MJS(\Psi air)}$), the ETo_{MJS} method was more sensitive to seasonal and regional climate heterogeneity.

Our validation results showed the higher association and agreement between $ETo_{MJS(\Psi air)}$ vs ETo_{LIS} (R = 0.76 and "*d*" index = 0.80) and ETo_{MJS} vs ETo_{LIS} (R = 0.75 and "*d*" index = 0.75), using the coefficients "*a*" and "*b*" described above. Even the highest error of adjustment obtained for ETo_{MJS} (MAE = 0.65 mm d^{-1}) resulted in low overestimations based on direct ETo_{LIS} measurements (<10%; Table 5). Since *VPD* is thought to has great influence on *ETo* in dry and warm conditions [36], the best performance of $ETo_{MJS(\Psi air)}$ is consistent with expected responses in semi-arid regions. As hypothesized, for such dry and warm climates, the best performance of $ETo_{MJS(\Psi air)}$ shows that Ψ_{air} and monthly average coefficients "*a*" and "*b*" grouped into climate subgroups, can be used to estimate *ETo* more confidently than in previous simplified models.

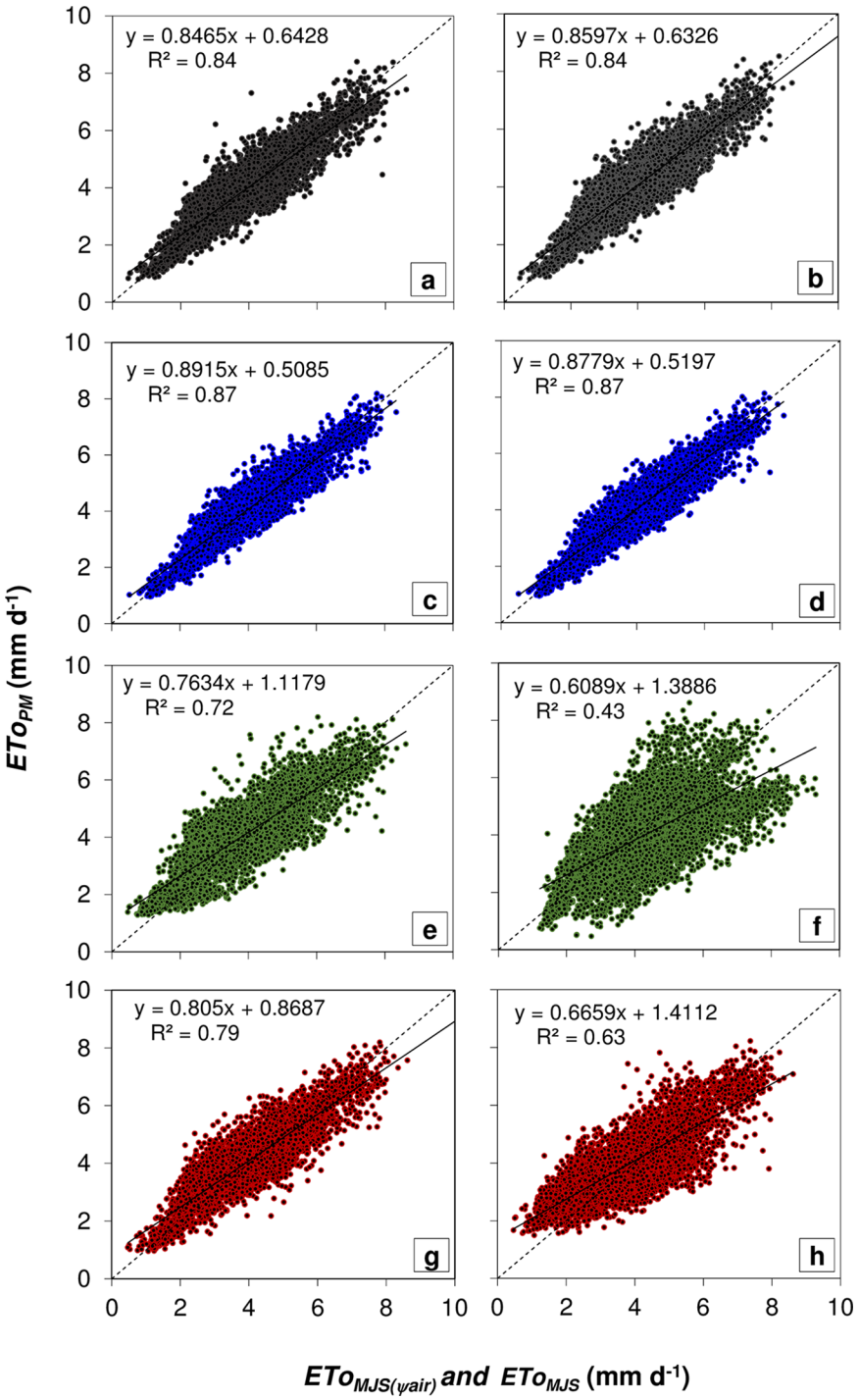

Fig 2. Daily reference evapotranspiration estimated by Penman-Monteith method as a response of reference evapotranspiration estimated between 2012 and 2014, considering different monthly "*a*" and "*b*" coefficients for each climate type for (a) $ETo_{MJS(\psi air)}$ and (b) ETo_{MJS}; different monthly average "*a*" and "*b*" coefficients for each climate subgroup for (c) $ETo_{MJS(\psi air)}$ and (d) ETo_{MJS}; different seasonal average "*a*" and "*b*" coefficients for each climate subgroup for (e) $ETo_{MJS(\psi air)}$ and (f) ETo_{MJS}; and, different annual average "*a*" and "*b*" coefficients for each climate subgroup for (g) $ETo_{MJS(\psi air)}$ and (h) ETo_{MJS}.

https://doi.org/10.1371/journal.pone.0180055.g002

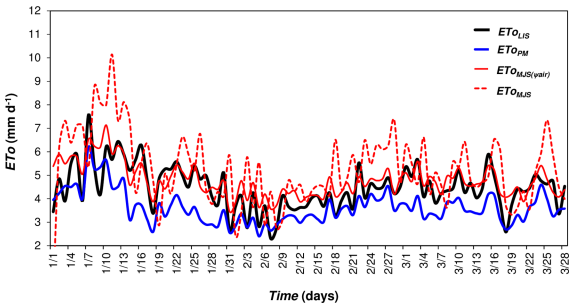

Fig 3. Daily ETo_{LIS}, ETo_{PM}, $ETo_{MJS(\Psi air)}$ and ETo_{MJS} for the semi-arid climate type *Bsh*, between 1997 and 1998 used as an in situ method of validation.

https://doi.org/10.1371/journal.pone.0180055.g003

Comparing the findings in this study with previous tests of alternative *ETo* methods in other climatic regions, our $ETo_{MJS(\Psi air)}$ method also resulted in higher association and agreement with the standard ETo_{PM}. For example, in tropical climate with dry winters (*Aw*) we obtained stronger agreement than previous simplifications based on either *RH* and air temperature (R = 0.49 to 0.83; "*d*" index = 0.49 to 0.69) [76] or based on solar radiation alone (R = 0.83, "*d*" index = 0.75) [40]. In addition, the association between ETo_{PM} and our alternative *ETo* estimates was stronger than those previously performed using *RH* and air temperature in other parts of the world [14, 73–75]. Methods based on solar radiation have been reported as a good alternative to the Penman-Monteith method either in humid [33, 51, 54, 77–79] and semi-arid climates [74, 80]. As it stands, these models present some difficulty of measurement [1, 5] due to scarce direct measurements and resulting large errors [31–32]. In our analysis, however, we show that even the sole use of Ψ_{air} in the alternative $ETo_{MJS(\Psi air)}$ method is sufficiently robust to estimate *ETo* in tropical and semi-arid climates. Moreover, the use of the solar radiation (*Ra*) in our method has proven to further improve *ETo* estimates, regardless of across all climatic zones studied here. Finally, the monthly average coefficients for climate subgroups improved the estimated ETo_{MJS}, such that the results indicate the possibility of using of the monthly average "*a*" and "*b*" coefficients to expand the geography of estimates and assess the potential of land-to-air water losses across different climatic zones (Fig 2C and 2D).

Taking into account the well-known limitations of the existing alternative methods [81], such as applicability in regions of strong seasonality of across regions of that encompass multiple climates [10, 12, 81], another important improvement of the proposed method is its sensitivity to spatial variability of climate conditions. The use of the Ψ_{air}–based estimates allows for investigating the spatial variability of *ETo*, which necessary to both conserve limited water resources as well as maintain food and energy production under changing climates [82–84].

Conclusions

In this study, we present a new model to estimate reference evapotranspiration in tropical and subtropical regions, where the climatic information needed for the standard *ETo* calculation is

Table 5. Performance of $ETo_{MJS(\Psi air)}$ and ETo_{MJS} relative to measured ETo_{LIS} for the semi-arid climate type *Bsh* in an annual basis, between 1997 and 1998.

Adjustment	R	"d" Index	MAE	MR
	(dimensionless)		(mm d^{-1})	(dimensionless)
$ETo_{MJS(\Psi air)}$ vs ETo_{LIS}	0.76	0.80	0.38	1.06
ETo_{MJS} vs ETo_{LIS}	0.75	0.75	0.65	1.10

https://doi.org/10.1371/journal.pone.0180055.t005

scarce or absent. We describe how geographical and seasonal variability in evapotranspiration can be accurately predicted based on radiation and atmospheric water potential estimates. The new simplified method is particularly robust in tropical and semi-arid climates, but can also be applied in subtropical and wet climates. In all cases, the new method has significant benefits with respect to accuracy and spatiotemporal scale of application relative to previous models. Continued measurements of air temperature and relative humidity (needed for Ψ_{air} modeling) across different land uses will improve the accuracy of land-to-air water flux estimates in future studies.

Supporting information

S1 Fig. Daily reference evapotranspiration estimated by Penman-Monteith method as a response of atmospheric water potential (Ψ_{air}), between 2004 and 2011, for the climate types: (a) Af; (b) Am; (c) As; (d) Aw; (e) Bsh; (f) Cfa; (g) Cfb; (h) Cwa; and, (i) Cwb.
(TIF)

S2 Fig. Daily reference evapotranspiration estimated by Penman-Monteith method as a response of $ETo_{MJS(}\Psi_{air)}$, between 2012 and 2014, for the climate types: (a) Af; (b) Am; (c) As; (d) Aw; (e) Bsh; (f) Cfa; (g) Cfb; (h) Cwa; and, (i) Cwb.
(TIF)

S3 Fig. Daily reference evapotranspiration estimated by Penman-Monteith method as a response of equivalent water evaporation (E_e), between 2004 and 2011, for the climate types: (a) Af; (b) Am; (c) As; (d) Aw; (e) Bsh; (f) Cfa; (g) Cfb; (h) Cwa; and, (i) Cwb.
(TIF)

S4 Fig. Daily reference evapotranspiration estimated by Penman-Monteith method as a response of ETo_{MJS} alternative method, between 2012 and 2014, for the climate types: (a) Af; (b) Am; (c) As; (d) Aw; (e) Bsh; (f) Cfa; (g) Cfb; (h) Cwa; and, (i) Cwb.
(TIF)

Author Contributions

Conceptualization: Daniela Jerszurki, Jorge L. M. Souza.

Data curation: Daniela Jerszurki, Jorge L. M. Souza.

Formal analysis: Daniela Jerszurki, Jorge L. M. Souza.

Funding acquisition: Daniela Jerszurki.

Investigation: Daniela Jerszurki.

Methodology: Daniela Jerszurki, Jorge L. M. Souza.

Project administration: Daniela Jerszurki.

Resources: Daniela Jerszurki.

Software: Daniela Jerszurki.

Supervision: Daniela Jerszurki, Jorge L. M. Souza, Lucas C. R. Silva.

Validation: Daniela Jerszurki.

Visualization: Daniela Jerszurki, Lucas C. R. Silva.

Writing – original draft: Daniela Jerszurki, Lucas C. R. Silva.

Writing – review & editing: Daniela Jerszurki, Lucas C. R. Silva.

References

1. Silva LCR. From air to land: understanding water resources through plant-based multidisciplinary research. Trends in Plant Sciences. 2015; 20: 399–401.
2. Blaney HF, Criddle WD. Determining Water Requirements in Irrigated Area from Climatological Irrigation Data. US Department of Agriculture: Soil Conservation Service; 1950.
3. Xu CY, Singh VP. Evaluation of three complementary relationship evapotranspiration models by water balance approach to estimate actual regional evapotranspiration in different climatic regions. Journal of Hidrology. 2005; 308: 105–121.
4. Schlesinger WH, Jasechko S. Transpiration in the global water cycle. Agricultural and Forest Meteorology. 2014; 189–190: 115–117.
5. Xavier AC, King CW, Scanlon BR. Daily gridded meteorological variables in Brazil (1980–2013). International Journal of Climatology. 2015; 36: 2644–2659.
6. Allen RG, Pereira LS, Raes D, Smith M. Crop evapotranspiration: guidelines for computing crop water requirements. 1.ed. Rome: Food and Agriculture Organization of the United Nations; 1998.
7. Carvalho LGC, Rios GFA, Miranda WL, Castro Neto P. Reference evapotranspiration: current analysis of different estimating methods. Pesquisa Agropecuária Tropical. 2011; 41:456–465.
8. Penman HL. Natural evaporation from open water, bare soil and grass. Proceedings of the Royal Society Serie B. 1948; 193: 120–145.
9. ASCE-EWRI. The ASCE standardized reference evapotranspiration equation. In: Allen RG, Walter IA, Elliott RL, Howell TA, Itenfisu D, Jensen ME, et al. editors. Report 0-7844-0805-X. American Society of Civil Engineers, Environmental Water Resources Institute; 2005. 69 p.
10. Jensen ME, Burman RD, Allen RG. Evapotranspiration and irrigation water requirements. New York: ASCE; 1990.
11. Hargreaves GH, Allen RG. History and evaluation of Hargreaves evapotranspiration equation. Journal of Irrigation and Drainage Engineering. 2003; 129: 53–63.
12. Thornthwaite CW. Report of the committee on transpiration and evaporation. Transactions of the American Geophysical Union. 1944; 25: 686–693.
13. Hamon WR. Estimating potential evapotranspiration. Journal of Hydraulics Division ASCE. 1961; 87: 107–120.
14. Romanenko VA. Computation of the autumn soil moisture using an universal relationship for a large area. In: Proceedings, Ukrainian Hydrometeorological Research Institute. 3 Kiev, 1961.
15. Turc L. Water requirements assessment of irrigation, potential evapotranspiration: simplified and updated climatic formula. Annals of Agronomy. 1961; 12: 13–49.
16. Jensen ME, Haise HR. Estimating evapotranspiration from solar radiation. Journal of the Irrigation and Drainage Division. 1963; 4: 15–41.
17. Makkink GF. Testing the Penman formula by means of lysimeters. Journal of the Institution of Water Engineers. 1957; 11: 277–288.
18. Schendel U. Vegetations Wasserverbrauch und Wasserbedarf. Habilitation, Kiel; 1967.
19. Benevides JG, Lopez D. Formula para el calculo de la evapotranspiracion potencial adaptada al tropico (15˚ N—15˚ S). Agronomia Tropical. 1970; 20: 335–345.
20. Campbell S. An Introduction to Environmental Biophysics. Springer, New York; 1977.
21. Priestley CHB, Taylor RJ. On the assessment of surface heat flux and evaporation using large-scale parameters. Monthly Weather Review. 1972; 100: 81–92.
22. Budiko MI. Climate and Life. New York: Academic; 1974.
23. Linacre ET. A simple formula for estimating evapotranspiration rates in various climates, using temperature data alone. Agricultural Meteorology. 1977; 18: 409–424.
24. Hargreaves GH, Samani ZA. Reference crop evapotranspiration from temperature. Applying Engineering Agriculture. 1985; 1: 96–99.
25. Trabert W. Neue Beobachtungenuber Verdampfungsgeschwindigkeiten. Meteorologische Zeitschrift. 1896; 13: 261–263.
26. Alexandris S, Kerkides P. New empirical formula for hourly estimations of reference evapotranspiration. Agricultural Water Management. 2003; 60: 157–180.

27. Trajkovic S. Hargreaves versus Penman-Monteith under Humid conditions. Journal of Irrigation and Drainage Engineering. 2007; 133: 38–42.
28. Ravazzani G, Corbari C, Morella S, Gianoli P, Mancini M. Modified Hargreaves-Samani equation for the assessment of reference evapotranspiration in Alpine River Basins. Journal of Irrigation and Drainage Engineering. 2012; 138: 592–599.
29. Valiantzas DJ. Simplified forms for the standardized FAO-56 Penman-Monteith reference evapotranspiration using limited data. Journal of Hydrology. 2013; 505: 13–
30. Berti A, Tardivo G, Chiaudani A, Rech F, Borin M. Assessing reference evapotranspiration by the Hargreaves method in north-eastern Italy. Agricultural Water Management. 2014; 140: 20–25.
31. Weiss A, Hays CJ, Hu Q, Easterling WE. Incorporating bias error in calculating solar irradiance: implications for crop simulations. Agronomy Journal. 2001; 93: 1321–1326.
32. Trajkovic S, Kolakovic S. Evaluation of reference evapotranspiration equations under humid conditions. Water Resources Management. 2009; 23: 3057–3067.
33. Martinez CJ, Thepadia M. Estimating reference evapotranspiration with minimum data in Florida, USA. Journal of Irrigation and Drainage Engineering. 2010; 136: 494–501.
34. Rojas JP, Sheffield RE. Evaluation of daily reference evapotranspiration methods as compared with the ASCE EWRI Penman-Monteith equation using limited weather data in northeast Louisiana. Journal of Irrigation and Drainage Engineering. 2013; 139: 285–292.
35. Todorovic M, Karic B, Pereira LS. Reference evapotranspiration estimate with limited weather data across a range of Mediterranean climates. Journal of Hydrology. 2013; 481: 166–176.
36. Rana G, Katerji N. A measurement based sensitivity analysis of the Penman-Monteith actual evapotranspiration model for crops of different height and in contrasting water status. Theoretical and Applied Climatology. 1998; 60: 141–149.
37. Camargo AP, Sentelhas PC. Performance evaluation of different methods of estimation of potential evapotranspiration in State of São Paulo. Revista Brasileira de Agrometereologia. 1997; 5: 89–97.
38. Silva KO, Miranda JH, Duarte SN, Folegatti MV. Análise de métodos de estimativa de evapotranspiração na otimização de sistemas de drenagem. Revista Brasileira de Engenharia Agrícola e Ambiental. 2005; 9: 161–165.
39. Borges AC, Mendiondo EM. Comparison of empirical equations to estimate reference evapotranspiration in Jacupiranga River Basin. Revista Brasileira de Engenharia Agrícola e Amiental. 2007; 11: 293–300.
40. Oliveira RA, Tagliaferre C, Sediyama GC, Materam FJV, Cecon PR. Performance of the "Irrigâmetro" in the estimation of reference evapotranspiration. Revista Brasileira de Engenharia Agrícola e Ambiental. 2008; 12: 166–173.
41. Syperreck VLG, Klosowski ES, Greco M, Furlanetto C. Avaliação de desempenho de métodos para estimativas de evapotranspiração de referência para a região de Palotina, Estado do Paraná. Acta ScientiarumAgronomy. 2008; 30: 603–609.
42. Borges VP, Oliveira AS, Coelho Filho MA, Silva TSM, Pamponet BM. Evaluating models for estimationofincoming solar radiation in Cruz das Almas, Bahia, Brazil Revista Brasileira de Engenharia Agrícola e Ambiental. 2010; 14: 74–80.
43. Pilau FG, Battisti R, Somavilla L, Righi EZ. Desempenho de métodos de estimativa da evapotranspiração de referência nas localidades de Frederico Westphalen e Palmeira das Missões—RS. Ciência Rural. 2012; 42: 283–290.
44. Cunha PCR, Nascimento JL, Silveira PM, Alves Júnior J. Efficiency of methods for calculating class A pan coefficients to estimate reference evapotranspiration. Pesquisa Agropecuária Tropical. 2013; 43: 114–122.
45. Lacerda ZC, Turco JEP. Estimation methods of reference evapotranspiration (ETo) for Uberlândia—MG. Engenharia Agrícola. 2015; 35: 27–38.
46. Tanaka AA, Souza AP, Klar AE, Silva AC, Gomes AWA. Evapotranspiração de referência estimada por modelos simplificados para o Estado do Mato Grosso, Brasil. Pesquisa Agropecuaria Brasileira. 2016; 51: 91–104.
47. Cunha FF, Magalhaes FF, Castro MA, Souza EJ. Performance of estimative models for daily reference evapotranspiration in the city of Cassilândia, Brazil. Engenharia Agrícola. 2017; 37: 173–184.
48. Vescove HV, Turco JEP. Comparação de três métodos de estimativa da evapotranspiração de referência para a região de Araraquara—SP. Engenharia Agrícola. 2005; 25: 713–721.
49. Melo GL, Fernandes ALT. Evaluation of empirical methods to estimate reference evapotranspiration in Uberaba, State of Minas Gerais, Brazil. Engenharia Agrícola. 2012; 32: 875–888.

50. Chagas RM, Faccioli GG, Aguiar Netto AO, Sousa IF, Vasco AN, Silva MG. Comparação entre métodos de estimativa da evapotranspiração de referência (ETo) no município de Rio Real-BA. Irriga. 2013; 18: 351–363.
51. Irmak S, Payero JO, Martin DL, Irmak A, Howell TA. Sensitivity analyses and sensitivity coefficients of standardized daily ASCE-Penman-Monteith equation. Journal of Irrigation and Drainage Engineering. 2006; 132: 564–578.
52. Lemos Filho LCA, Mello CR, Faria MA, Carvalho LG. Spatial-temporal analysis of water requirements of coffee crop in Minas Gerais State, Brazil. Revista Brasileira de Engenharia Agrícola e Ambiental. 2010; 14: 165–172.
53. Silva AO, Moura GBA, Silva EFF, Lopes PMO, Silva APN. Análise espaço-temporal da evapotranspiração de referência sob diferentes regimes de precipitações em Pernambuco. Revista Caatinga. 2011; 24: 135–142.
54. Hupet F, Vanclooster M. Effect of the sampling frequency of meteorological variables on the estimation of reference evapotranspiration. Journal of Hydrology. 2001; 243: 192–204.
55. Gong L, Xu C, Chen D, Halldin S, Chen YD. Sensitivity of the Penman-Monteith reference evapotranspiration to key climatic variables in the Changjiang (Yangtze River) basin. Journal of Hydrology. 2006; 329: 3–4.
56. Yan H, Wang SQ, Billesbach D, Oechel W, Zhang JH, Meyers T, et al. Global estimation of evapotranspiration using a leaf area index-based surface energy and water balance model. Remote sensing of environment. 2012; 124: 581–595.
57. Hillel D. Soil and water: physical principles and processes. Academic press: New York; 1971.
58. Reichardt K, Timm LC. Solo, planta e atmosfera: conceitos, processos e aplicações. 2ed. Barueri: Manole; 2012.
59. Silva LCR, Pedroso G, Doane TA, Mukome FND, Horwath WR. Beyond the cellulose: Oxygen isotope composition of plant lipids as a proxy for terrestrial water balance. Geochemical Perspectives Letters. 2015; 1: 33–42.
60. Kämpfer N. Monitoring Atmospheric Water Vapor. Ground-based Remote Sensing and In-situ Methods. 1ed. Springer: New York; 2013.
61. Philip JR. Sources and transfer processes in the air layers occupied by vegetation. Journal of Applied Meteorology. 1964; 3: 390–395.
62. Slayter RO. Plant-water relationships. Academic Press, London; 1967.
63. Novák V. Evapotranspiration in the Soil-Plant-Atmosphere System. Springer Science and Business Media: New York, London; 2013.
64. INMET–Brazilian National Institute of Meteorology. Meteorological Database for Education and Research (BDMEP). 2014. Available: http://www.inmet.gov.br/portal/index.php?r=bdmep/bdmep
65. Álvares CA, Stape JL, Sentelhas PJ, Gonçalves JLM, Sparovek G. Koppen's climate classification map for Brazil. Meteorologische Zeitschrift. 2013; 22: 711–728.
66. Murray FW. On the computation of saturation vapor pressure. Journal of Applied Meteorology. 1967; 6: 203–204.
67. Wright JL, Jensen ME. Peak water requirements of crops in southern Idaho. Journal of Irrigation and Drainage Engineering. 1972; 98: 193–201.
68. Medeiros AT. Reference evapotranspiration estimated by Penman-Monteith equation, lysimetric measures and empirical equations in Paraipaba, State of Ceara, Brazil. M. Sc. Thesis, Piracicaba: Escola Superior de Agricultura "Luiz de Queiroz". 2002.
69. Willmott CJ, Ackleson SG, Davis JJ, Feddema KM, Klink DR. Statistics for the evaluation and comparison of models. Journal of Geophysical Research. 1985; 90: 8995–9005.
70. Wilks DS. Statistical Methods in the Atmospheric Sciences. 3. ed. Academic Press: Oxford, UK and Waltham, MA; 2011.
71. Alexandris S, Kerkides P, Liakatas A. Daily reference evapotranspiration estimates by the "Copais" approach. AgriculturalWater Management. 2006; 86: 371–386.
72. Pandey PK, Dabral PP, Pandey V. Evaluation of reference evapotranspiration methods for the northeastern region of India. International Soil and Water Conservation Research. 2016; 4: 52–63.
73. Djaman K, Balde AB, Sow A, Muller B, Irmak S, N'Diaye MK, et al. Evaluation of sixteen reference evapotranspiration methods under sahelian conditions in the Senegal River Valley. Journal of Hydrology: regional studies. 2015; 3: 139–159.
74. Sabziparvar AA, Tabari H. Regional estimation of reference evapotranspiration in arid and semi-arid regions. Journal of Irrigation and Drainage Engineering. 2010; 136:724–731.

75. Mendonça JC, Sousa EF, Bernardo S, Dias GP, Grippa S. Comparison of estimation methods of reference crop evapotranspiration (ETo) for Northern Region of Rio de Janeiro State, Brazil. Revista Brasileira de Engenharia Agrícola e Ambiental. 2003; 7: 276–279.

76. Borges Junior JCF, Anjos RJ, Silva TJA, Lima JRS, Andrade CLT. Métodos de estimativa da evapotranspiração de referência diária para a microrregião de Garanhuns, PE. Revista Brasileira de Engharia Agrícola e Ambiental. 2012; 16: 380–390.

77. Yoder RE, Odhiambo LO, Wright WC. Evaluation of methods for estimating daily reference crop evapotranspiration at a site in the humid southeast United States. Applying Engineering Agriculture. 2005; 21: 197–202.

78. Gocic M, Trajkovic S. Software for estimating reference evapotranspiration using limited weather data. Computers and Eletronics in Agriculture. 2010; 71: 158–162.

79. George BA, Raghuwanshi NS. Inter-comparison of reference evapotranspiration estimated using six methods with data from four climatological stations in India. Journal of Indian Water Resources Society. 2012; 32: 15–22.

80. Mohawesh OE. Evaluation of evapotranspiration models for estimating daily reference evapotranspiration in arid and semiarid environments. Plant, Soil and Environment. 2011; 57: 145–152.

81. Penman HL. Evaporation, transpiration and evapotranspiration. In: Vegetation and hydrology. Farnham Royal: Common wealth Agricultural Bureaux; 1963.

82. Duursma RA, Kolari P, Perämäki M, Nikinmaa E, Hari P, Delzon S, et al. Predicting the decline in daily maximum transpiration rate of two pine stands during drought based on constant minimum leaf water potential and plant hydraulic conductance. Tree Physiology. 2008; 28: 265–276. PMID: 18055437

83. Gharun M, Turnbull TL, Henry J, Adams MA. Mapping spatial and temporal variation in tree water use with an elevation model and gridded temperature data. Agricultural Forest Meteorology. 2015; 200: 249–257.

84. Couvreur V, Kandelous MM, Sanden BL, Lampinen BD, Hopmans JW. Downscaling transpiration rate from field to tree scale. Agricultural and Forest Meteorology. 2016; 221: 71–77.